

Modeling of damage in cement paste subject to external sulfate attack

Chuansheng Xiong¹, Linhua Jiang^{*1,2}, Yan Zhang¹ and Hongqiang Chu¹

¹College of Mechanics and Materials, Hohai University, 1 Xikang Rd., Nanjing, China

²National Engineering Research Center of Water Resources Efficient Utilization and Engineering Safety, 1 Xikang Rd., Nanjing, China

(Received August 13, 2015, Revised December 12, 2015, Accepted December 16, 2015)

Abstract. This study aimed to develop models of sulfate diffusion and ettringite content profile in cement paste for the predication of the damage behavior in cement paste subject to external sulfate. In the models, multiphase reaction equilibrium between ions in pore solution and solid calcium aluminates phases and the microstructure changes in different positions of cement paste were taken into account. The distributions of expansive volume strain and expansion stress in cement paste were calculated based on the ettringite content profile model. In addition, more sulfate diffusion tests and SEM analyses were determined to verify the reliability and veracity of the models. As the results shown, there was a good correlation between the numerical simulation results and experimental evidences. The results indicated that the water to cement ratio (w/c) had a significant influence on the diffusion of sulfate ions, ettringite concentration profile and expansion properties in cement paste specimens. The cracking points caused by ettringite growth in cement paste specimens were predicted through numerical methods. According to the simulation results, the fracture of cement paste would be accelerated when the specimens were prepared with higher w/c or when they were exposed to sulfate solution with higher concentration.

Keywords: modeling; sulfate diffusion; ettringite profile; volume strain; cement paste

1. Introduction

Sulfate attack is a vital reason in the degradation of concrete structures (Neville 2004). When concrete is exposed to external sulfate-laden environments, sulfate ions can penetrate into the hardened concrete voids owing to the concentration gradient between the interior and exterior of concrete. After that, the penetrated sulfate ions react with cement hydrates, forming various chemical compounds (i.e., gypsum, ettringite etc.) with larger volume. Then, the expansion occurs with the growth of the newly formed expansive compounds (Gospodinov *et al.* 1996, 1999, 2007a, b). Microcracks generate and develop with the growth of expansion stress when it reaches a certain value, destroying the exposed concrete layer by layer.

*Corresponding author, Professor, E-mail: lhjiang@hhu.edu.cn

Over the past couple of decades, efforts had been made to develop models that can be used to predict the diffusion process of sulfate ions in concrete (Idiart *et al.* 2011, Tixier and Mobasher 2003a, b, Bonakdar *et al.* 2012, Zuo *et al.* 2012). Most of the models were based on the Fick's second law, with consideration of the influences of chemical reactions and the formation of expansive products, but few reasonable and sufficient experimental evidences had been given to certify them (Gospodinov *et al.* 1996, 1999, 2007a, b, Idiart *et al.* 2011, Tixier and Mobasher 2003a, b, Bonakdar *et al.* 2012, Zuo *et al.* 2012). Up to now, it is difficult to choose a reasonable diffusion coefficient when modeling sulfate diffusion due to various conditions and limited results of experiments. In some previous models, the effective diffusivity was considered as a function of time and water/cement ratio (Tumidajski *et al.* 1995), and in others as a function of porosity and hydration degree of cements (Zuo *et al.* 2012, Sun *et al.* 2013). However, few of the models made a consideration of the effects of microstructure changes in different positions of concrete, let alone gave the analyses of multiphase reaction equilibrium in sulfate diffusion process, such as the ionic interactions between solid aluminates phases and liquid phases. In fact, the concentration of others ions (Ca^{2+} and OH^-) and solid calcium aluminates phases have great influences on the diffusion and dissipation of sulfate ions in concrete (Gospodinov *et al.* 2007a, b, Peng *et al.* 2006, Prince *et al.* 2003, Diamidot and Glasser 1993). Moreover, the effects of porosity changes on diffusion coefficient of SO_4^{2-} were not sufficiently considered in previous models, failing to reflect the nature of sulfate diffusion behavior in concrete. Also, most papers mainly focused on the modeling of sulfate ion diffusion, ignoring the simulation of ettringite diffusion and its expansion profile in concrete subjected to external sulfate attack which is also meaningful for the evaluation of concrete durability.

In this paper, models of sulfate diffusion and ettringite profile in cement paste were developed, in which the multiphase reaction equilibrium between ions in pore solution and solid calcium aluminates phases and the microstructure variations in different positions of cement paste were taken into account. The distributions of volume strain and expansion stress in cement paste were calculated based on the ettringite concentration profile model. In addition, more sulfate diffusion tests and SEM analyses were determined to verify the reliability and veracity of the models.

2. Mathematical modeling of sulfate diffusion

2.1 Sulfate diffusion in cement paste and the effective diffusion coefficient

As is known to all, hardened cement paste is a porous body, containing capillaries, gel pores and microcracks, seen in Fig. 1, where, the capillaries can be considered as the main transmitting channels of ions. The C-S-H matrix is usually thought to be impassable for ions, but to be consumed by chemical reaction (Koukkari and Pajarre 2007). The diffusion of sulfate into cement paste not only changes the composition of ions in pore solutions, but also causes the variations of microstructures owing to the formation of gypsum or/and ettringite. At the same time, the variations of microstructures in hardened cement paste can also effect the diffusion of sulfate ions (Bary *et al.* 2014, Garboczi 1990, Garboczi and Bentz 1992, Page *et al.* 1981). Thus, we might introduce a new parameter "pore geometry factor" to account for the influences of pore structures and the variations on the diffusion coefficient of sulfate ions. Then, the effective diffusion coefficient can be expressed as

$$D_{eff} = k_{\phi} D_0 \quad (1)$$

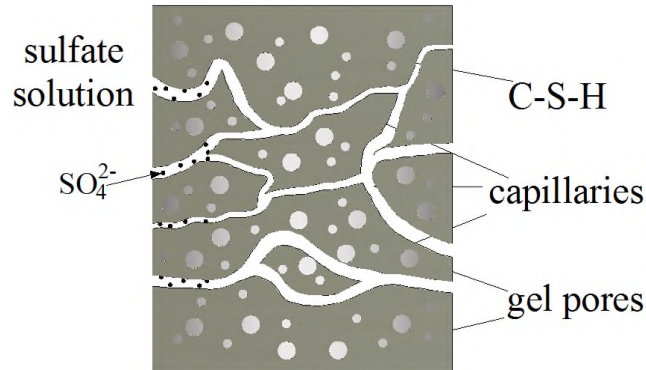


Fig. 1 Schematic diagram of diffusing process of sulfate ions

where k_φ is the “pore geometry factor”, which is mainly associated with the porosity of capillaries. D_{eff} is the effective diffusion coefficient of sulfate ions. D_0 is the diffusion coefficient of sulfate ions in ideal solution, the value of which is $1.07 \times 10^{-9} \text{ m}^2/\text{s}$ in water solution at 25°C .

In fact, however, the capillary system of cement stone is very complicated like a disordered net, which is made up plenty of capillaries with different characteristics. Sulfate penetration would experience various pore paths with different tortuosity and porosity (Koukkari and Pajarre 2007). For simplification, the diffusion paths of sulfate ions with different tortuosity are integrated as a vertical path to the attacked surface. The tortuosity of capillaries can be expressed as τ . The value of τ is 1/3 by considering the diffusivity of ions in capillaries is along three directions. Thus, the parameter k_φ can be written as

$$k_\varphi = \frac{\varphi(x,t)}{\tau} \tag{2}$$

where $\varphi(x, t)$ is the capillary porosity in cement paste. In the diffusion process of sulfate ions, the capillary porosity will be changed due to the hydration of cement and the formation of gypsum or/and ettringite. Then, the porosity of cement paste can be written as

$$\varphi(x,t) = f(x,t) \cdot \varphi_0 \tag{3}$$

with the $f(x, t)$ is the filling rate of capillary porosity by the formation of ettringite. Therefore, we might assume that the filling rate $f(x, t)$ is related to the quantity of chemically reacted sulfate ions, and is in the range of 0 to 1. Then, we may write Eq. (4)

$$f(x,t) = (1 - k_c \cdot C)^\beta \quad \text{if } k_c \cdot C < 1 \text{ (and 1 otherwise)} \tag{4}$$

where k_c and β are empirical coefficient, representing the filling rate of capillary. C is the concentration of sulfate ions in pore solution. In addition, the initial capillary porosity φ_0 of cement paste is primarily associated with the water to cement ratio and the degree of cement hydration. Through Powers’ model, the φ_0 can be calculated by

$$\varphi_0 = \frac{w/c - 0.36\alpha}{w/c + 0.32} \quad \text{if } w/c > 0.36\alpha \text{ (and 0 otherwise)} \tag{5}$$

where w/c is the water to cement ratio, and α is the degree of cement hydration. Thus, through Eq. (1) and relations (2), (3) and (4), we obtain the equation of the effective diffusion coefficient of sulfate ions in cement paste, shown as

$$D_{eff} = \frac{[1 - k_c \cdot C]^\beta \cdot \varphi_0 \cdot D_0}{\tau} \quad (6)$$

here, D_{eff} is a function related to the exposing time t , the depth x and the concentration of sulfate ions C in pore solutions.

2.2 Multiphase reaction equilibrium and the reaction rates

It is assumed that cement paste specimens are exposed to solutions with sulfate sodium. When sulfate ions penetrate into the cement paste, a series of reactions between solid phases in the cement paste and ions in pore solution can happen. In this process, gypsum forms in the first step, and then ettringite (AFt) follows, crystallizing and expanding, as shown in Fig. 2.

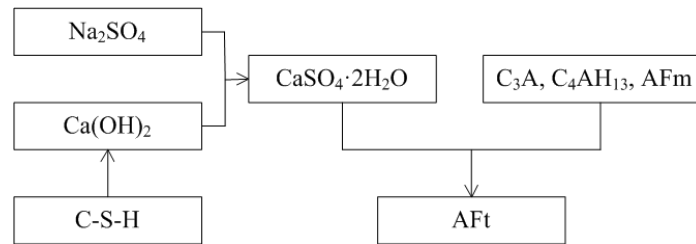
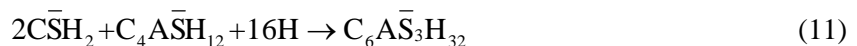
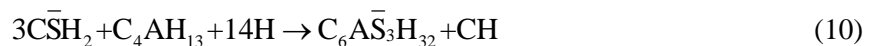


Fig. 2 the diagram of ettringite formation process in concrete exposed to sodium sulfate

The classical mechanisms of sodium sulfate attack on hardened cement paste can be summarized in the following reactions (Idiart *et al.* 2011, Tixier and Mobasher 2003a, b)



where, the CH, CSH_2 , C3A, C4AH13, $\text{C}_4\text{ASH}_{12}$, H and $\text{C}_6\text{AS}_3\text{H}_{32}$ are calcium hydroxide, gypsum, tricalcium aluminate, tetracalcium aluminate hydrate, monosulfoaluminate (AFm), hydrone and ettringite. Seen from the equations above, both the diffusion and chemical reactions can lead to the changes of sulfate content, cement hydrates and attacking products. However,

owing to the low diffusion rate of the solid phases (like gypsum, ettringite and other aluminates), only ions diffusion were considered when modeling the process. Moreover, it is assumed that the calcium aluminates phases are mainly three components (C_3A , C_4AH_{13} , $C_4A\bar{S}H_{12}$) and enough for the sulfate consuming reactions, as the Eq. (9)-(11) shown. In previous studies (Idiart *et al.* 2011, Tixier and Mobasher 2003a, b, Bonakdar *et al.* 2012, Zuo *et al.* 2012), these reactions had often been simplified and lumped in a global sulfate phase-aluminate phase reaction as



where C_a was an equivalent grouping of the reacting calcium aluminates, and q represented the weighted average stoichiometric coefficient of the lump reaction. The penetrating sulfate ions were considered to be consumed by a second-order chemical reaction. Gospodinov (1996, 1999 and 2007a, b) and Bonakdar (2012), then, investigated the chemical reactions as 1st order terms. However, according to the chemical reaction thermodynamics, the formation of ettringite in fact proceeds by steps in liquid phase. There are some drawbacks to use the rate of chemical reaction to replace the depletion rate of sulfate ions while ignoring the influences of the concentration of coexisting ions in pore solution of concrete. To overcome this, the formation of ettringite is best to be described using an ionic equation (Peng *et al.* 2006).



This does not mean that the reactants of ettringite are essentially species dissolved in water. It just indicates that the formation and stability of ettringite are closely related to the concentration of SO_4^{2-} , AlO_2^- , Ca^{2+} , and OH^- , in order of $Ca^{2+} > OH^- > SO_4^{2-} > AlO_2^-$ (Peng *et al.* 2006). According to chemical reaction kinetics, the formation rate of ettringite is equal to the difference between the positive reaction rates (dissolution rates or desorption rates) and the negative reaction rates (formation rates or absorption rates) (Diamidot and Glasser 1993). Therefore, the reaction rate of Eq. (13) can be written as

$$r = k_a^{ett} \cdot \{ [Ca^{2+}]^6 \cdot [OH^-]^4 \cdot [AlO_2^-]^2 \cdot C^3 \}^n - k_d^{ett} \cdot S_{ett} \tag{14}$$

where r is the reaction rate of formation of ettringite, S_{ett} is the efficient surface area of ettringite, k_a^{ett} and k_d^{ett} are respectively the decomposition rate and formation rate of ettringite, n is the reaction order. Both of the positive and the negative reaction rates are obtained from the mass conservation law. In these formats, though they might not completely accord with the realistic kinetics, the reactions could immediately approximate to the thermodynamic equilibrium state. In the process of actual calculation of reaction rate, the surface area of ettringite cannot be accurately expressed. Then, to simplify the calculation, here, we assume the surface area of ettringite is direct proportional to its content in cement paste. The values of parameters k_a^{ett} , k_d^{ett} and n have to be determined by inverse analysis. Here, we can use the empirical values when calculating a practical example.

It is assumed that the diffusion of sulfate in cement paste doesn't change the pH value of pore solution and the pore solution of cement paste is kept as saturated solution of calcium hydroxide. Then, the concentration of OH^- can be calculated by the pH value, shown as

$$[OH^-] = 10^{pH-14} \tag{15}$$

According to the solubility product constant of $Ca(OH)_2$, the $[Ca^{2+}]$ can be obtained from the following equation

$$[\text{Ca}^{2+}] = \frac{k_{sp,0}^{CH}}{[\text{OH}^-]^2} \quad (16)$$

where $k_{sp,0}^{CH}$ is the solubility product constant of $\text{Ca}(\text{OH})_2$.

Furthermore, in pore solution of hardened cement paste, the AlO_2^- is mainly provided by calcium aluminates phases. Therefore, the $[\text{AlO}_2^-]$ in Eq. (14), in fact, represents the effective specific surface area of solid phases of aluminates. The same as the S_{ett} , the $[\text{AlO}_2^-]$ is mainly impacted by the quantity of Al_2O_3 in cement and the capillary porosity. Then, we may write Eq. (17).

$$[\text{AlO}_2^-] = k_A \cdot \varphi_0 \cdot C_A \quad (17)$$

where k_A is the proportionality coefficient, C_A is the quantity of Al_2O_3 in cement.

Through Eq. (14) and relations Eq. (15)-(17), the reaction rate of formation of ettringite can be expressed as

$$r = k_a^{ett} \cdot \left[\frac{(k_{sp,0}^{CH})^6 \cdot k_A^2 \cdot \varphi_0^2 \cdot C_A^2 \cdot C^3}{10^{8 \cdot (\text{pH}-14)}} \right]^n - k_d^{ett} \cdot C_{ett} \quad (18)$$

where C_{ett} is the content of ettringite formed in cement paste. Then, the absorbed amount of sulfate ions per unit time can be obtained as

$$R = 3 \cdot r \quad (19)$$

where R is the adsorption rate of sulfate concentration in concrete per unit volume due to the chemical reactions.

2.3 The governing equation and boundary conditions

Based on the Fick's law and the law of mass conservation, one can write the 1-D governing equation of sulfate ions in cement paste, shown as

$$\frac{\partial(D_{eff} \cdot \frac{\partial C}{\partial x})}{\partial x} = \frac{\partial C}{\partial t} + R \quad (20)$$

where C is the concentration of sulfate ions in pore solution, t is exposing time, x is the distance from the exposing surface.

To define the boundary and initial conditions, it can be assumed that the initial porosity of cement paste is φ_0 and the sulfate concentration in exposing solution is C_s . Then, the boundary conditions are

$$C(x,t) = \begin{cases} \frac{\varphi_0 \cdot C_s \cdot \rho_s}{M_{NS}}, & x=0, t \in [0, \infty) \\ 0, & x \rightarrow \infty, t \in [0, \infty) \end{cases} \quad (21)$$

where M_{NS} is the molar mass of sodium sulfate, ρ_s is the density of pore solution.

The 1-D governing equation of ettringite content formed in cement paste can be written as

$$\frac{\partial C_{ett}}{\partial t} = r \tag{22}$$

for which, the boundary conditions are

$$C_{ett}(x,t) = \begin{cases} 0, & x = 0, t \in [0, \infty) \\ 0, & x \rightarrow \infty, t \in [0, \infty) \end{cases} \tag{23}$$

3. Analysis of the chemo-mechanical model

3.1 Calculation of expansion strain

Up to now, it is fairly well accepted that ettringite is the main cause for the expansions, and in most of previous models, ettringite has often been proposed to be responsible for the expansive process (Idiart *et al.* 2011, Tixier and Mobasher 2003a, b, Bonakdar *et al.* 2012, Garboczi 1990, Basista and Weglewski 2008). However, the mechanisms of expansions for concrete exposed to sulfate attack are still controversial. For instance, when the humidity of concrete drops to a certain level, gypsum will not continue to react with aluminates phases to form ettringite whether the aluminates phases are run out or not, but to crystallize on capillary walls, fill the capillaries and cause expansion. To clarify this, a great deal of tests measurements need to be done.

Here, to simplify the calculation process, the following assumptions are made:

- (1) The cement paste is water-saturated.
- (2) Gypsum will continue to react with aluminates phases to form ettringite if the aluminates phases were not run out.

Hence, ettringite can be considered to be the only reaction products and govern the expansion of cement paste samples. Then, based on the previous models (Idiart *et al.* 2011, Tixier and Mobasher 2003a, b), the volumetric change due to the formation of ettringite from different aluminates can be written as

$$\begin{cases} \frac{\Delta V_i}{V_i} = \frac{M^{ett}}{M^A + a_A \cdot M^{gyp}} - 1 \\ M^i = \frac{m^i}{\rho^i} \end{cases} \tag{24}$$

where M^A is the molar volume of each species of aluminates, M^{ett} and M^{gyp} are the molar volume of ettringite and gypsum, a_A is the stoichiometric coefficient involved in each reaction, seen in Eq. (9) to (11), m^i is the molar mass of different species, ρ^i is the density of of different species. The values of m^i and ρ^i of different species are listed in Table 1. The values of $\Delta V_i/V_i$ for different aluminates phases can be calculated by Eq. (24), shown in Table 2.

Thus, in previous studies (Idiart *et al.* 2011, Tixier and Mobasher 2003a, b), the reporters have proposed that the expansion of cement paste matrix per unit volume could be obtained by the

Table 1 Values of m^i and ρ^i of different species

Species	ρ^i (g/cm ³)	m^i (g/mol)	M^i (cm ³ /mol)
C ₃ A	3.04	270	88.82
C ₄ AH ₁₃	2.02	560	277.23
C ₄ A \bar{S} H ₁₂	1.95	622	318.97
C \bar{S} H ₂	2.32	172	74.14
C ₆ A \bar{S} ₃ H ₃₂	1.75	1254	716.57

Table 2 Values of volume change for each reaction

Reaction cases	$\Delta V_i/V_i$
Eq. (9)	1.302
Eq. (10)	0.434
Eq. (11)	0.533

calculation the reacted quantity of different calcium aluminates phases (which was reported to be calculated by the content of initial calcium aluminates and the content of unreacted calcium aluminates). However, as is known to all, the cement hydration is a complex physico-chemical procedure; the cement hydrates are also diverse with all kinds of phases. Hence, it is difficult and unnecessary to differentiate the concentration of the different calcium aluminates phases in cement paste, let alone to calculate the reacted part. Furthermore, there are not just calcium aluminates phases in cement paste matrix. The quantity of other phases, such as C-S-H gel and pore structures, also impacts the volume change of the entirety. Therefore, to simplify the calculation process, we might consider the expansion of cement paste matrix per unit volume is proportional to the quantity of chemical formed ettringite, then, we can write Eq. (25)

$$\Delta \varepsilon_v^{ett} = k_v \cdot \frac{C_{ett}}{\sum_i c_i} \quad (25)$$

in which C_{ett} is the concentration of ettringite newly formed, which can be obtained by the Eq. (22). The proportionality k_v is in fact the expansion strain caused by the formation of ettringite per unit mole, relating to the initial proportion of different aluminates phases, which can be assumed to be associated to the degree of hydration and the initial quantity of gypsum in cement paste, expressed as

$$k_v = \sum_{i=1}^n \frac{\Delta V_i}{V_i} \cdot \frac{c_i}{\sum_i c_i} = (1-\alpha) \cdot \frac{\Delta V_1}{V_1} + \alpha \cdot \left(1 - \frac{c_{gyp}}{\sum_i c_i}\right) \cdot \frac{\Delta V_2}{V_2} + \alpha \cdot \frac{c_{gyp}}{\sum_i c_i} \cdot \frac{\Delta V_3}{V_3} \quad (26)$$

where c_{gyp} is the initial quantity of cement paste. Before causing the volume change in cement paste, ettringite may first fill a fraction of the capillary porosity. It is assumed that the filling rate is $f(x,t)$. For concrete, the value of $f(x,t)$ is in the range of 0.05 to 0.40 ((Idiart *et al.* 2011), while for cement paste, the range may be changed. Then, the total volumetric strain can be obtained as

$$\Delta\varepsilon_v = \Delta\varepsilon_v^{ett} - f(x,t) \cdot \varphi_0 \quad \text{with } \Delta\varepsilon_v^{ett} > f(x,t) \cdot \varphi_0 \text{ (and 0 otherwise)} \quad (27)$$

Correspondingly, it is assumed that cement paste is isotropy, then, the linear strain can be calculated by

$$\Delta\varepsilon = \frac{1}{3} \Delta\varepsilon_v \quad (28)$$

3.1 Constitutive relation and cracking judgment criteria of cement paste

Generally, the damage process of cementitious materials depends on the properties, internal structures, deformation characteristics, cracks, expansion process, and the accumulation of internal damage, etc. The damage of cement paste exposed to sodium sulfate is due to formation of expansion stress caused by the expansive ettringite. To calculate the expansion stress of cement paste, we may take the expansion strain as tensile strain of concrete. The corresponding expansion stress can be calculated by the constitutive relation of concrete under uniaxial stretch. Guo and Shi (2003) proposed the sectional form of complete stress-strain curve equation of concrete under uniaxial stretch, which can be expressed as

$$\frac{\sigma}{f_t} = \begin{cases} 1.2\gamma - 0.2\gamma^6, & \gamma \leq 1 \\ \frac{\gamma}{0.312f_t^2(\gamma-1)^{1.7} + \gamma}, & \gamma > 1 \end{cases} \quad (29)$$

in which σ is expansion stress of cement paste, f_t is the ultimate tensile stress of cement paste, and γ is the relative deformation value, shown as

$$\gamma = \frac{\varepsilon}{\varepsilon_t} \quad (30)$$

where ε_t is the ultimate tensile strain of cement paste. Then, we may define the cracking judgment criteria of cement paste under sulfate attack as; in view of the inherent defects in cement paste, if $\sigma \geq 0.8f_t$, then the cement paste is cracked.

Table 3 Composition of cement (wt. %)

Compn.	SiO ₂	Al ₂ O ₃	Fe ₂ O ₃	CaO	MgO	Na ₂ O	K ₂ O	others
Content	23.74	5.01	5.12	61.93	1.22	0.51	0.87	0.40

Table 4 Material parameters used in simulation models

α	0.9	τ	1/3
M_{NS} (g/mol)	142.06	k_c (m ³ /mol)	0.01
ρ_s (g/mm ³)	1.05	β	2
k_a^{ett} (s ⁻¹)	6.5×10^{-7}	k_A	1
k_d^{ett} (s ⁻¹)	1.1×10^{-15}	ε_t	1×10^{-4}
n	1	f_t (MPa)	1.0
pH	12.5	ρ_c (g/mm ³)	2.0

4. Experiments and related parameters

4.1 Materials and experiments

To verify the applicability of the theoretical model applied above, cement paste specimens were exposed to sodium sulfate solution for different periods of time. The P. II 42.5 cement (GB 175-2007) was used for preparing the cement paste. The composition of the cement is listed in Table 3. The water to cement ratio of cement paste are 0.35, 0.4, 0.45, 0.5 and 0.55. Specimens prepared for the measurement of sulfate distribution profile were circular columns with a size of $\phi 50 \text{ mm} \times 100 \text{ mm}$. After curing for 91 days in standard conditions, two end surfaces of the samples were coated with epoxy resin, and then were kept in solutions of Na_2SO_4 with concentrations of 3%, 5%, 8% and 10% by weight. The concentration profile of sulfate was determined at exposing time of 60 days, 180 days, 360 days, 540 days and 720 days. The sulfate concentrations at different depths in the specimens were obtained by using a method of drilling. Powder samples were taken from the cement paste layer by layer from the exposed surface to internal. The chemical method of EDTA complexometric titration (GB/T13025.8-1991) was used to measure the sulfate content in the specimens (Sun *et al.* 2003). In addition, the SEM analyses were done to confirm the accuracy of the numerical simulation with the models. For SEM tests, samples were prepared by cutting specimens from the deteriorated portion, dried using an oven and then coated with gold before testing.

4.2 Parameters for the model

Seen from the models above, many chemical reaction kinetics theories and parameters can be found. However, most of the reaction rates, coefficients or parameters have not been reported in any handbooks of chemistry or previous studies. It is also difficult to be obtained by routine experimental analyses. Some existing data of these parameters in existing models were just given to fit some specific or controlled experimental evidences, or the true models. Probably, they are not so perfectly suitable in another place. Therefore, based on the cement paste specimens used in the above experiments and some existing experiences (Gospodinov *et al.* 1996, 1999, 2007a, b, Idiart *et al.* 2011, Tixier and Mobasher 2003a, b, Bonakdar *et al.* 2012, Zuo *et al.* 2012a, b, Bary *et al.* 2014, Bassuoni and Nehdi 2008, Song *et al.* 2014, Feng *et al.* 2014), the parameters used in the simulation of cement paste are given in Table 4.

5. Experimental results and numerical simulations

5.1 Profiles of sulfate ions in cement paste

Fig. 3 shows the simulation and experimental results of sulfate concentration profiles for different time (60days, 180days, 360days, 540days and 720days) in specimens exposed to 5% Na_2SO_4 solution. It can be seen from Fig 3 that the content of sulfate on the surface of cement paste specimens achieves a high value in short order. With the increasing of depth, it is significantly reduced. As time goes by, sulfate ion concentrations at different positions increase, and the closer to the exposed surface the higher of the sulfate ion concentration is. Comparing with Fig. 3(a) and Fig. 3(b), it can be found that w/c impacts much on the diffusion rate of sulfate ions,

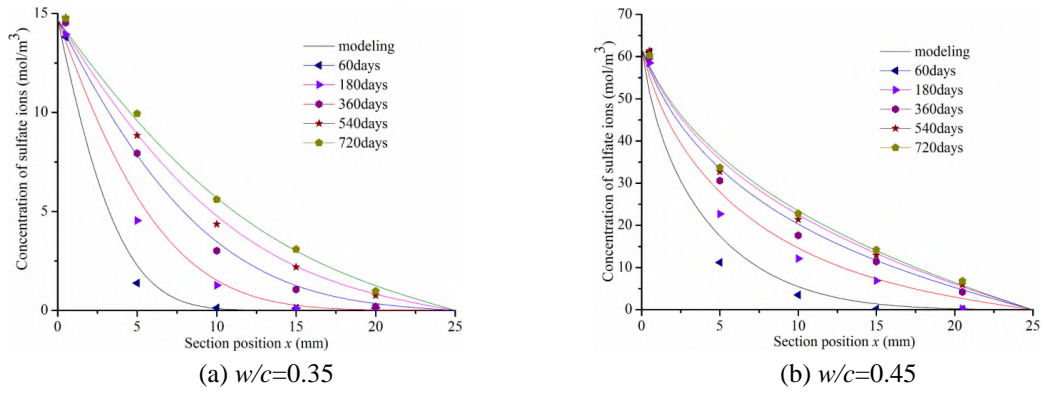


Fig. 3 Sulfate concentration profiles of different times in specimens exposed to 5% NaSO₄ solution

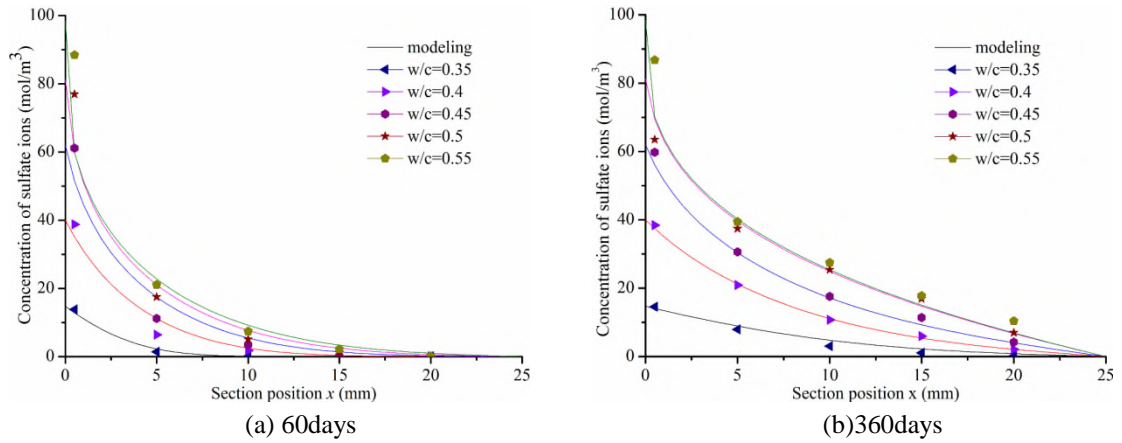


Fig. 4 Sulfate concentration profiles in specimens with different w/c exposed to 5% NaSO₄ solution

especially in the late period. Seen from the experimental results and the modeling results, there is a good relevance between them. This indicates that the model can suit the experiments well, and the further proof will be given below.

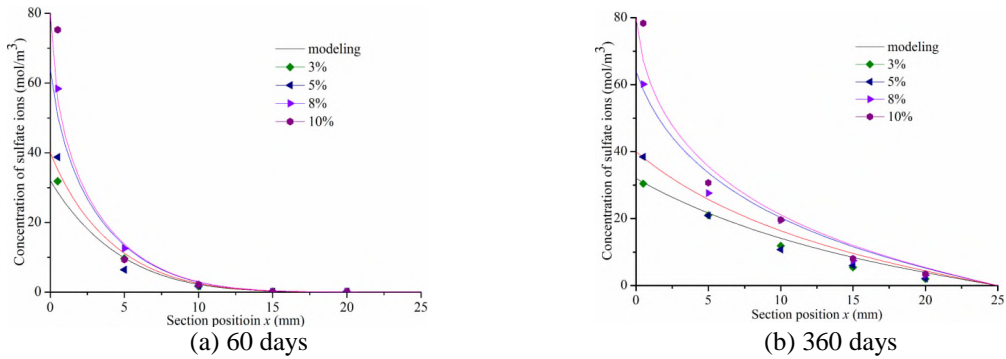


Fig. 5 Sulfate concentration profiles in specimens with w/c=0.4 exposed to different solution

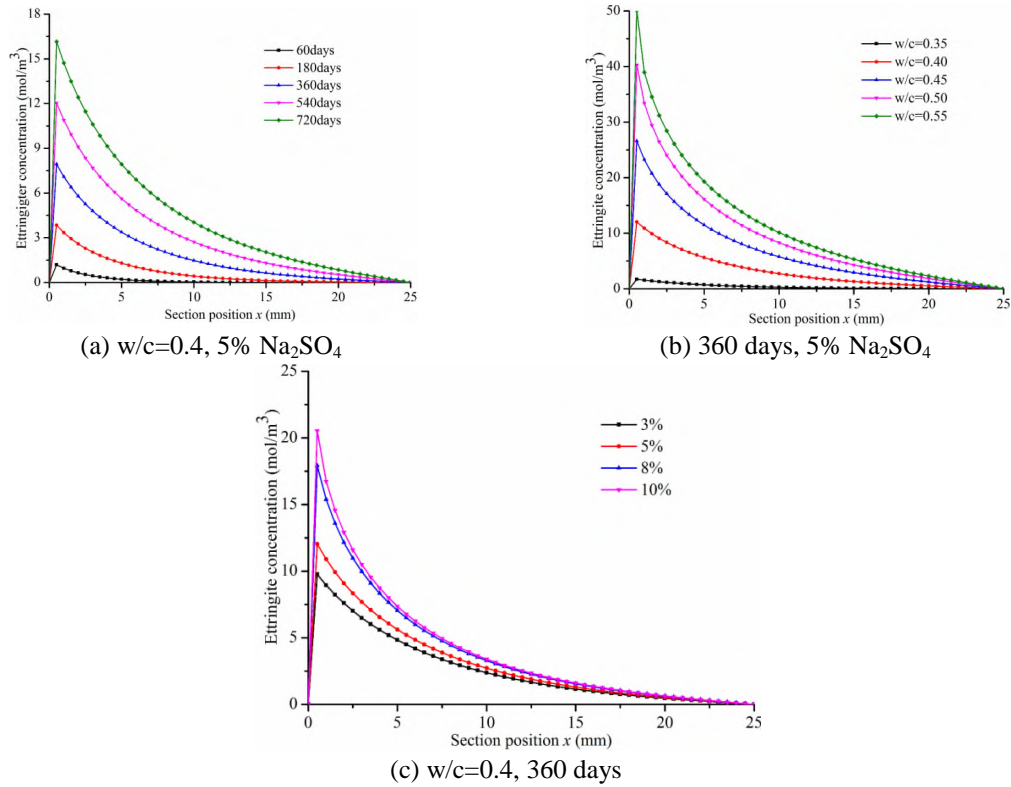


Fig. 6 Etringite concentration profile in specimens with controlled conditions

Fig. 4 gives the simulation and experimental results of sulfate concentration profiles in specimens with different w/c (0.35, 0.40, 0.45, 0.50 and 0.55). Seen from Fig. 4(a) and (b), obvious influences of w/c on the surface concentrations of sulfate ions can be found. With the increasing of w/c , the surface concentrations of sulfate ions have a significantly increase due to the increase of capillary porosity. With the increasing of the depth, the sulfate ion concentrations reduce rapidly, and the large the w/c is the more quickly the concentrations reduce. This may be due to the formation of expansive ettringite and the filling of capillaries near the surface position. Therefore, to some extent, the influences of w/c on sulfate ion diffusion in internal of specimens are weakened. In addition, comparing with the experimental results and the simulation results, a reasonable approximation can be found between them, especially for the specimens with lower w/c .

Fig. 5 shows the simulation and experimental results of sulfate concentration profiles in specimens with $w/c=0.4$ exposed to sodium sulfate water solutions with different concentrations (3%, 5%, 8% and 10%). It can be seen from the figures that the concentrations of source solutions mainly impact the surface sulfate ion concentration and the diffusion rate of sulfate ions in internal cement paste specimens. Obviously, the surface sulfate ion concentration increases with more sodium sulfate in source solution, and is affected little by the exposing time. For the internal of the specimens, the influences of source solution are weakened owing to the filling of capillaries near the exposed surface with newly formed expansive ettringite. The weakened degree increases with

the growth of sulfate concentration in source solution, because of the faster formation rate of ettringite with high concentration of sulfate ions. Still, it is obvious in the figures that the sulfate concentration profiles are closely related to the experimental data.

5.2 Ettringite concentration profile

Fig. 6 presents the simulation of ettringite concentration profiles in specimens with different numerical conditions. It can be found that the surface concentration of ettringite is about 0 mol/m^3 due to the dissolution of Ca^{2+} on the exposed surface. No gypsum will be generated at the position where there are no Ca^{2+} ions in the pore solution. In addition, ettringite will also be disintegrated where the concentration of Ca^{2+} ions is low. This result is similar to that obtained by Samson and Marchand (2007). In the position near from the exposed surface, the penetrated sulfate ions react with Ca^{2+} to form gypsum and continue to generate ettringite. As time goes by, more ettringite forms with more sulfate ions penetrating into the cement paste. At the same time, the position of the border of ettringite formation on the section moves to the internal. It can be seen from Fig. 6(b) that the ettringite concentration is significantly increased with the addition of w/c. The reason is twofold: one is that the larger w/c allows more sulfate ions to penetrate into cement paste, meanwhile, it also increases the diffusion rate of sulfate ion; the other is that the crystallization of ettringite is formed in capillaries; the larger w/c provides more capillaries where ettringite is generated.

In the sense of chemical reaction kinetics, it increases the chances of contact between sulfate ions and calcium aluminates phases with a large w/c. Compared with the influence of w/c on ettringite formation, the sodium sulfate concentration in source solution seems have less influences. Seen from Fig. 6(c), the sodium sulfate concentration is increased from 3% to 10%, whereas, the ettringite concentration of 360 days near the exposed surface is changed from 10 mol/m^3 to 20.5 mol/m^3 , much smaller than that of w/c from 1.5 mol/m^3 to 50 mol/m^3 . This indicates that a reasonable w/c is very important to resistance of sulfate attack of concrete.

Fig. 7 shows the SEM pictures of specimens with different positions. Seen from Fig. 7(a), no morphology of ettringite is found on the exposed surface of specimens. This provides the evidences of that the concentration of ettringite on the surface of cement paste specimens is 0 mol/m^3 . According to the simulation results, much ettringite is generated near the exposed surface. This also accords with the results of SEM analysis. As shown in Fig. 7(b), many needle materials can be found in the specimens at the position of 2.5mm to 5mm from the exposed surface. With the addition of depth, the ettringite concentration decreases, seen from Fig. 7(c). This is because of that sulfate ions have not penetrated into those places. The observation of the small number of ettringite is due to the gypsum brought by cement.

5.3 Distribution of volume strain and expansion stress in cement paste

Fig. 8 shows the simulation of volume strain profiles in specimens with different numerical conditions. Seen from the figures, it is easy to find that the changing rules of volume strain in specimens are very similar to that of the ettringite concentration in Fig. 6. At the beginning of the diffusion of sulfate ions, the volume strain approximates to zero, because the existed capillaries are needed to be filled for a certain degree by ettringite crystal before the expansion occurs.

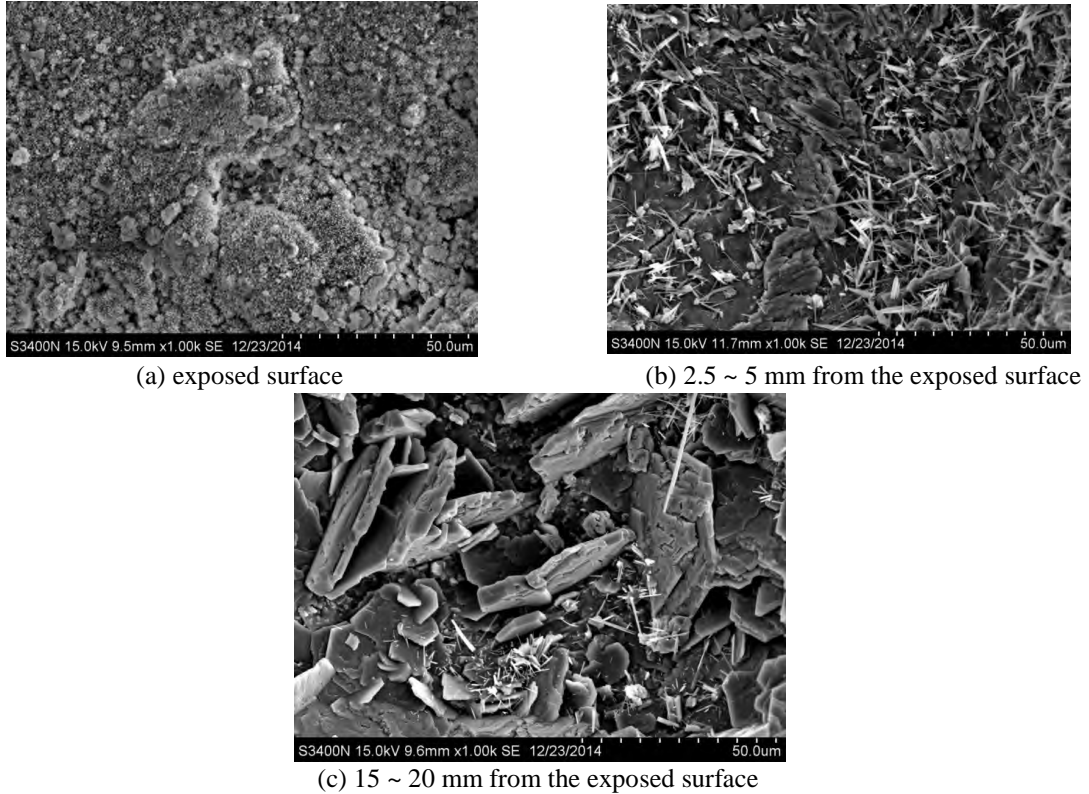
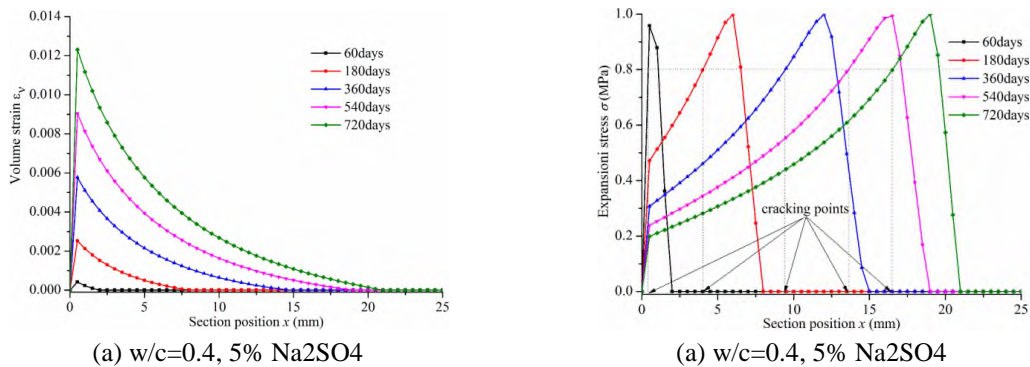
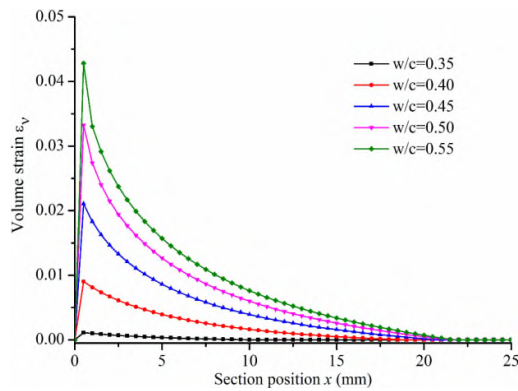


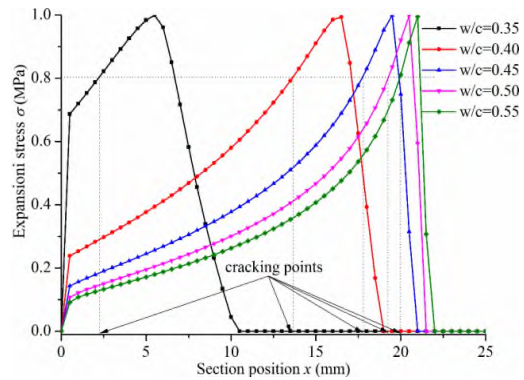
Fig. 7 SEM pictures of specimens with different positions

As the time goes by, the expansion volume strain increases with the growth of ettringite crystal. It can be seen from Fig. 8(b) that the w/c has significantly influences on the expansion volume strain in specimens, especially in the positions near the exposed surface. This is also equivalent to the influences of w/c on the ettringite concentration profiles. Then, it can be obtained that the expansion volume strain profile in specimens is closely related to the quantity of ettringite in cement paste. Likewise, the sodium sulfate concentration in source solution does not much affect volume strain profiles in specimens.

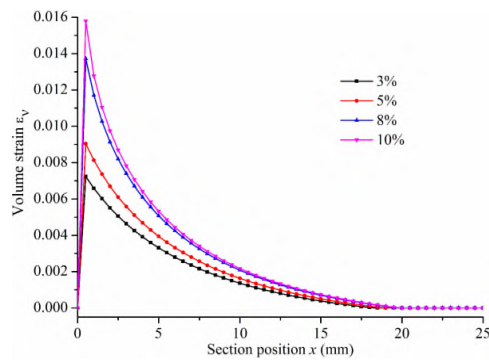




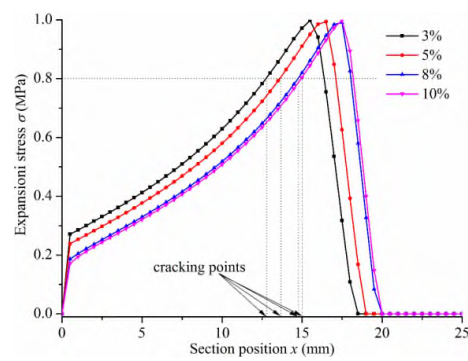
(b) 360 days, 5% Na₂SO₄



(b) 360 days, 5% Na₂SO₄



(c) w/c=0.4, 360days



(c) w/c=0.4, 360days

Fig. 8 Volume strain profile produced by ettringite growth in specimens with controlled conditions

Fig. 9 Expansion stress profile and cracking points in specimens with controlled conditions

Fig. 9 presents the expansion stress profile and cracking points produced by ettringite growth in specimens with controlled conditions. Before the diffusion of sulfate ions, the initial strain in specimens is 0 MPa. With time going, the expansion stress increases due to the complete of the capillary filling with ettringite crystal, and the cracking occurs when it reaches to a certain value ($0.8f_t$). For example, seen from Fig. 9(a), the position of cracking point for 60 days is 0.8 mm from the exposed surface, and that for 360 days is 12.8 mm. At the exposing time of 360 days, Fig. 9(b) shows the influences of w/c on the expansion stress. It can be found that there is an obvious increase of cracking point depth with the addition of w/c. This indicates that it not only restrains the diffusion of sulfate ions but also slows the movement speed of cracking points in specimens with lower w/c. The result is similar to the influence of w/c on the ettringite concentration profile and volume strain profile. Furthermore, the concentration of sodium sulfate in source solution has little influences on the distribution of expansion stress and the change of cracking position in cement paste specimens.

6. Conclusions

A numerical model of sulfate diffusion was developed for the predication of sulfate concentration profile in cement paste. In which, the multiphase reaction equilibrium between ions in pore solution and solid calcium aluminates phases and the microstructure variations in different positions of cement paste were taken into account. The comparisons between the simulated and experimental results showed that the w/c of cement paste had great influences on the diffusion process of sulfate ions because of the change of initial capillary porosity with w/c. The sulfate concentration in source solution has little effect on sulfate diffusion in cement paste expect for the surface concentration of sulfate.

A model of ettringite content profile in cement paste was proposed to calculate the distributions of volume strain and expansion stress in cement paste. In the basis of which, the cracking points produced by ettringite growth in cement paste specimens were predicted. As the results shown, be similar to the influences of w/c and the sulfate concentration of the source solution on sulfate diffusion in cement paste, the formation rate of ettringite and the growth rate of expansion stress were quicker when the cement paste were prepared with higher w/c or immersed in source solution with higher sulfate concentration. Correspondingly, the cement paste would be cracked earlier when the specimens were prepared with higer w/c or when they were exposed to source solution with higher sulfate concentration.

Acknowledgments

The research described in this paper was financially supported by the National Key Technology Research and Development Program of the Ministry of Science and Technology of China (No. 2015BAB07B04), the National Natural Science Foundation of China (No. 51278167 and 51479551).

References

- Bary, B., Leterrier, N., Deville, E. and Bescop, P.L. (2014), "Coupled chemo-transport-mechanical modelling and numerical simulation of external sulfate attack in mortar", *Cement Concrete Comp.*, **49**(5), 70-83.
- Basista, M. and Weglewski, W. (2008), "Micromechanical modeling of sulphate corrosion in concrete: influence of ettringite forming reaction", *Theor. Appl.Mech.*, **35**(2), 29-52.
- Bassuoni, M.T. and Nehdi, M.L. (2008), "Neuro-fuzzy based prediction of the durability of self-consolidating concrete to various sodium sulfate exposure regimes", *Comput. Concrete*, **5**(6), 573-597.
- Bonakdar, A., Mobasher, B. and Chawla, N. (2012), "Diffusivity and micro-hardness of blended cement materials exposed to external sulfate attack", *Cement Concrete Comp.*, **34**(1), 76-85.
- Diamidot, D. and Glasser F.P. (1993), "Thermodynamic investigation of the CaO-Al₂O₃-CaSO₄·2H₂O system at 25°C and the influence of Na₂O", *Cement Concrete Res.*, **23**(1), 221.
- Feng, P., Miao, C.W. and Bullard, J.W. (2014), "A model of phase stability, microstructure and properties during leaching of Portland cement binders", *Cement Concrete Comp.*, **49**, 9-19
- Garboczi, E.J. (1990) "Permeability, diffusivity, and microstructural parameters: a critical review", *Cement Concrete Res.*, **20**(9), 591-601.
- Garboczi, E.J. and Bentz, D.P. (1992), "Computer simulation of the diffusivity of cement-based materials", *J. Mater. Sci.*, **27**(8), 2083-2092.
- Gospodinov, P., Kazandjiev, R. and Mironova, M. (1996), "The effect of sulfate ion diffusion on the structure of cement stone", *Cement Concrete Comp.*, **18**(6), 401-407.

- Gospodinov, P.N., Kazandjiev, R.F., Partalin, T.A. and Mironova, M.K. (1999), "Diffusion of sulfate ions into cement stone regarding simultaneous chemical reactions and resulting effects", *Cement Concrete Res.*, **29**, 1591-1596.
- Gospodinov, P., Kazandjiev, R. and Mironova, M. (2007a), "Mechanisms of sulfate ionic diffusion in porous cement based composites", *Comput. Concrete*, **4**(4), 273-284.
- Gospodinov, P., Kazandjiev, R. and Mironova, M. (2007b), "Mechanisms of sulfate ionic diffusion in porous cement based composites: effect of capillary size change", *Comput. Concrete*, **4**(2), 273-284.
- Guo, Z.H. and Shi, X.D. (2003), *Theory and analysis of reinforced concrete*, Tsinghua University Press, Beijing, China.
- Idiart, A.E., López, C.M. and Carol, I. (2011), "Chemo-mechanical analysis of concrete cracking and degradation due to external sulfate attack: a meso-scale model", *Cement Concrete Comp.*, **33**(3), 411-423.
- Koukkari, P. and Pajarre, R. (2007), "Combining reaction kinetics to the multi-phase gibbs energy calculation", *Comput. Aided Chem. Eng.*, **24**(7), 153-158.
- Neville, A. (2004), "The confused world of sulfate attack on concrete", *Cement Concrete Res.*, **34**(8), 1275-1296.
- Page, C.L., Short, N.R. and Tarras, A.E. (1981), "Diffusion of chloride ions in hardened cement pastes", *Cement Concrete Res.*, **11**(3), 395-406.
- Peng, J.H., Zhang, J.X. and Qu, J. (2006), "The mechanism of formation and transformation of ettringite", *Journal of Wuhan University of Technology - Mater. Sci. Ed.*, **21**(3), 158-161.
- Prince, W., Espagne, M. and AiTcin, P.C. (2003) "Ettringite formation: a crucial step in cement superplasticizer compatibility", *Cement Concrete Res.*, **33**(5), 635-641.
- Samson, E. and Marchand, J. (2007), "Modeling the transport of ions in unsaturated cement-based materials", *Comput. Struct.*, **85**(23), 1740-1756.
- Song, Z., Jiang, L., Chu, H., Xiong, C., Liu, R. and You, L. (2014), "Modeling of chloride diffusion in concrete immersed in CaCl₂ and NaCl solutions with account of multi-phase reactions and ionic interactions", *Constr. Build. Mater.*, **66**(1), 1-9.
- Sun, C., Chen, J., Zhu, J., Zhang, M. and Ye, J. (2013), "A new diffusion model of sulfate ions in concrete", *Constr. Build. Mater.*, **39**(1), 39-45.
- Tixier, R. and Mobasher, B. (2003a), "Modeling of damage in cement-based materials subjected to external sulfate attack. i: formulation", *J. Mater. Civ. Eng.*, **15**(4), 305-313.
- Tixier, R. and Mobasher, B. (2003b), "Modeling of damage in cement-based materials subjected to external sulfate attack. ii: comparison with experiments", *J. Mater. Civ. Eng.*, **15**(4), 314-322.
- Tumidajski, P.J., Chan, G.W. and Philipose, K.E. (1995), "An effective diffusivity for sulfate transport into concrete", *Cement Concrete Res.*, **25**(6), 1159-1163.
- Zuo, X.B., Sun, W. and Yu, C. (2012a), "Numerical investigation on expansive volume strain in concrete subjected to sulfate attack", *Constr. Build. Mater.*, **36**(4), 404-410.
- Zuo, X.B., Sun, W., Li, H. and Zhao, Y.K. (2012b), "Modeling of diffusion-reaction behavior of sulfate ion in concrete under sulfate environments", *Comput. Concrete*, **10**(1), 79-93.